

Research Paper

Echogenic Glycol Chitosan Nanoparticles for Ultrasound-Triggered Cancer Theranostics

Hyun Su Min^{1*}, Dong Gil You^{1,2*}, Sejin Son¹, Sangmin Jeon^{1,2}, Jae Hyung Park², Seulki Lee³, Ick Chan Kwon^{1,4}, and Kwangmeyung Kim¹✉

1. Center for Theragnosis, Biomedical Research Institute, Korea Institute of Science and Technology (KIST), Hwarangno 14-gil 6, Seongbuk-gu, Seoul 136-791, South Korea
2. School of chemical engineering, Sungkyunkwan University, Suwon 440-746, South Korea
3. The Russell H. Morgan Department of Radiology and Radiological Science, Center for Nanomedicine at the Wilmer Eye Institute, Johns Hopkins School of Medicine, Baltimore, Maryland 21287, USA
4. KU-KIST School, Korea University, 1 Anam-dong, Seongbuk-gu, Seoul 136-701, South Korea

* Hyun Su Min and Dong Gil You are co-first authors.

✉ Corresponding author: Dr. Kwangmeyung Kim, Center for Theragnosis, Biomedical Research Institute, Korea Institute of Science and Technology (KIST), Hwarangno 14-gil 6, Seongbuk-gu, Seoul 136-791, South Korea. E-mail: Kim@kist.re.kr

© 2015 Ivyspring International Publisher. Reproduction is permitted for personal, noncommercial use, provided that the article is in whole, unmodified, and properly cited. See <http://ivyspring.com/terms> for terms and conditions.

Received: 2015.06.30; Accepted: 2015.08.30; Published: 2015.10.18

Abstract

Theranostic nanoparticles hold great promise for simultaneous diagnosis of diseases, targeted drug delivery with minimal toxicity, and monitoring of therapeutic efficacy. However, one of the current challenges in developing theranostic nanoparticles is enhancing the tumor-specific targeting of both imaging probes and anticancer agents. Herein, we report the development of tumor-homing echogenic glycol chitosan-based nanoparticles (Echo-CNPs) that concurrently execute cancer-targeted ultrasound (US) imaging and US-triggered drug delivery. To construct this novel Echo-CNPs, an anticancer drug and bioinert perfluoropentane (PFP), a US gas precursor, were simultaneously encapsulated into glycol chitosan nanoparticles using the oil in water (O/W) emulsion method. The resulting Echo-CNPs had a nano-sized particle structure, composing of hydrophobic anticancer drug/PFP inner cores and a hydrophilic glycol chitosan polymer outer shell. The Echo-CNPs had a favorable hydrodynamic size of 432 nm, which is entirely different from the micro-sized core-empty conventional microbubbles (1-10 μm). Furthermore, Echo-CNPs showed the prolonged echogenicity via the sustained microbubble formation process of liquid-phase PFP at the body temperature and they also presented a US-triggered drug release profile through the external US irradiation. Interestingly, Echo-CNPs exhibited significantly increased tumor-homing ability with lower non-specific uptake by other tissues in tumor-bearing mice through the nanoparticle's enhanced permeation and retention (EPR) effect. Conclusively, theranostic Echo-CNPs are highly useful for simultaneous cancer-targeting US imaging and US-triggered delivery in cancer theranostics.

Key words: theranostic nanoparticle, echogenicity, ultrasound imaging, ultrasound contrast agent, tumor targeting, drug delivery.

Introduction

Recent clinical cancer therapy still remains far from successful in spite of the constant attempts utilizing nanoparticles to overcome the adverse effects of conventional chemotherapy.[1-3] Although the use of nanoparticles has improved the tumor targeting of

anti-cancer drugs, the less than perfect tumor targeting efficiency of nano-sized delivery cargo has inevitably caused unsatisfactory therapeutic efficacy and toxicities in normal tissues and cells.[4-7] In this context, ultrasound (US) technologies in combination

with highly sophisticated echogenic particles deserve full credit as an effective means to ablate solid tumors very effectively.[8] This is because US can be focused and penetrate deeply at the target regions, improving the selectivity of the cancer imaging and treatment while reducing undesirable side effects immensely.[9] In addition, the US-induced biological effects become more powerful and beneficial when US energy interacts with oscillating echogenic particles. The cavitation is induced by the expansion, collapse and oscillation of bubbles that can be utilized as a sonoporation inducer for enhancing drug/gene penetration into tissues and cells.[8, 10-14]

With the advancement of US technologies, echogenic particles have been evolving now from a simple echo enhancer for US imaging to versatile echogenic particles, which are equipped with drug-loading, specific disease-targeting and *in vivo*-friendly physicochemical functions and features.[13,14] Because the inner gas is a poor solvent for drug molecules, effective drug-loading strategies must be employed in various ways. Up until now, conventional gas-filled microbubbles, which can be destroyed by US energy, have been applied to the localized and/or targeted drug delivery and the optimization of drug action.[15, 16] Nevertheless, conventional microbubbles are still incapable of specific tumor targeting, due to their large particle size and short half-life, which occurs within several minutes of being in the blood stream. Furthermore, these microbubbles also have poor drug loading capacity as a drug delivery carrier.[17-19]

Recently, new echogenic nanoparticles have attracted much attention, due to their unique properties of cancer-targeting US imaging and US-triggered drug delivery system in cancer treatment. In particular, echogenic lipid-based nanoparticles and polymeric micelles containing a specific type of US contrast agent of perfluoropentane (PFP, boiling temperature is 29°C) have been extensively explored as new US-based theranostic nanoparticles.[20-25] This is because PFP-encapsulated nanoparticles could present the temperature-dependent phase-transition property from liquid-phase PFP to microbubble formation at the body temperature.[21, 25] Therefore, PFP-encapsulated nanoparticles could be localized at the targeted tumor tissue through the enhanced permeability and retention (EPR) effect and the particles were transformed into micro-sized echogenic bubbles at tumor tissues. These microbubbles at targeted tumor tissues could be used as new echogenic particles for cancer-targeting US imaging and US-triggered drug delivery system in cancer theranostics. However, it has been reported that PFP-encapsulated nanoparticles still presented major problems, such as het-

erogeneous size distribution and short *in vivo* half-life, in the engineering of ideal nano-sized echogenic nanoparticles.[20-22]

Herein, we present new anticancer drug- and liquid-phase PFP-encapsulated echogenic glycol chitosan nanoparticles (Echo-CNPs) that have a homogeneous nano-sized particle structure for cancer theranostics. To develop novel echogenic and theranostic nanoparticles, an anticancer drug and bioinert perfluoropentane (PFP), an US gas precursor, were simultaneously encapsulated into pre-formulated tumor-homing glycol chitosan nanoparticles (CNPs) via the oil in water (O/W) emulsion method. We previously reported that the liquid-phase PFP was successfully encapsulated into the hydrophobic inner cores of pre-formulated hyaluronic acid nanoparticles using the O/W emulsion method, wherein the PFP in oil phase was simply and successfully encapsulated into pre-formulated hyaluronic acid nanoparticles in aqueous phase using a gentle sonication for 2 min at 0 °C.[26] This new approach of utilizing pre-formulated, self-assembled nanoparticles to encapsulate liquid-phase PFP provided several advantages in the construction of nano-sized, very stable and long-acting US contrast agents. Interestingly, the liquid-phase PFP was confined in multiple hydrophobic inner cores inside the hyaluronic acid nanoparticles. Therefore, the homogeneous nano-sized particle structure could be rationally engineered to go into the systemic blood circulation with the enhanced half-life and strong echogenicity in tumor-specific US imaging.

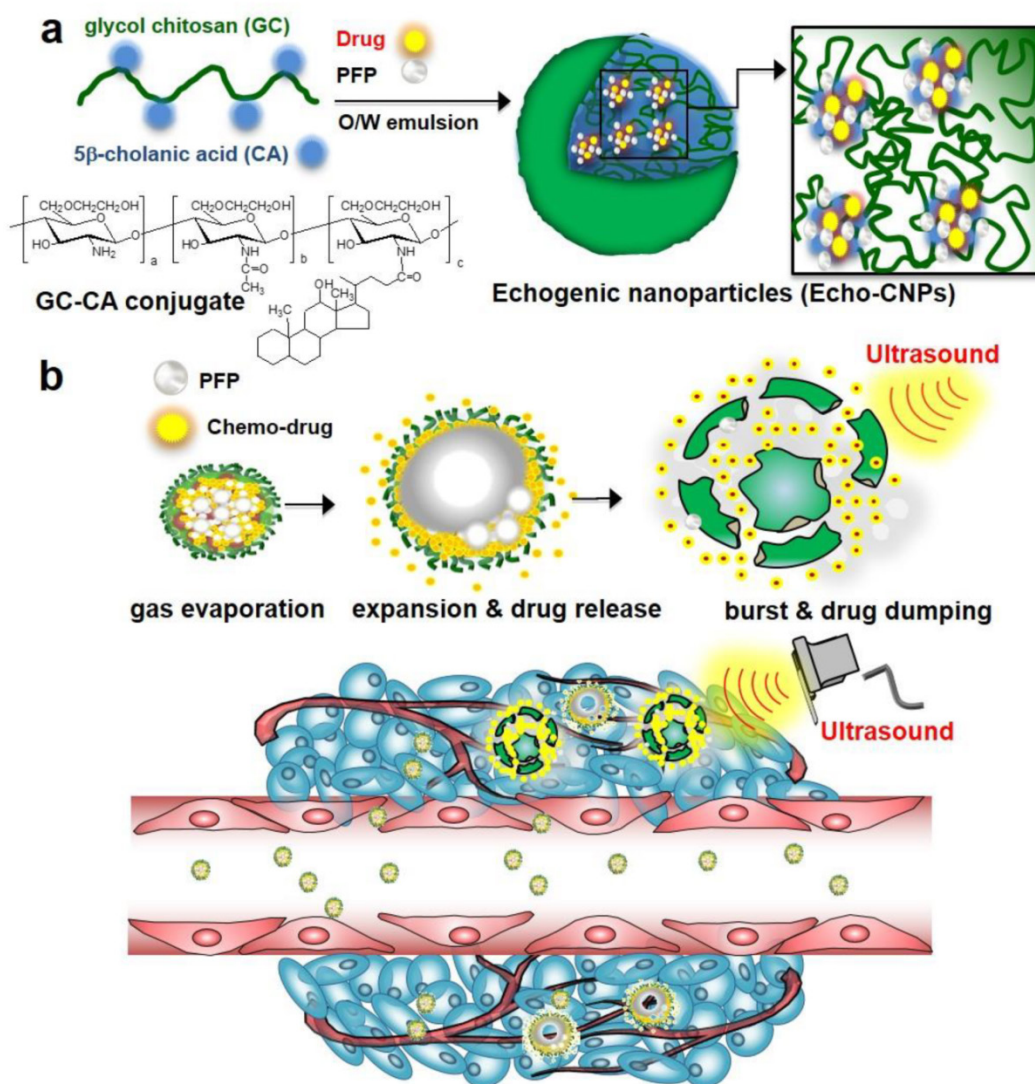
For cancer theranostics, by using this simple O/W emulsion method, pre-formulated and tumor-homing anticancer drug-encapsulated glycol chitosan nanoparticles (CNPs) with *in vivo* favorable nano-dimensions of 300 nm were used as robust and effective scaffold to encapsulate extremely hydrophobic and bioinert PFP into the hydrophobic inner cores of CNPs. The produced Echo-CNPs were composed of drug/PFP inner hydrophobic cores and biocompatible glycol chitosan outer shell, formulated via the oil in water (O/W) emulsion method. For tumor-targeting US imaging and US-triggered chemo-drug delivery, newly developed Echo-CNPs were designed to have *in vivo*-favorable physicochemical properties with the convenient nano-sized particle structure (432 nm), high drug-loading efficiency, prolonged echogenic properties, as well as tumor-specific tumor targeting, etc. Importantly, Echo-CNPs simultaneously containing both drug and PFP presented a high level of tumor accumulation, which may lead to successful cancer theranostics: US imaging and US-triggered drug delivery at the same time.

Results and Discussion

Rational Design of Drug and PFP Encapsulated Echo-CNPs

A new approach was made that pre-formulation of anticancer drug-encapsulated glycol chitosan nanoparticles (CNPs) was first prepared prior to the encapsulation of echogenic liquid-phase perfluoropentane (PFP).[26] Pre-formulated anticancer drug-encapsulated CNPs with *in vivo*-favorable nano-dimensions can provide a robust and effective scaffold to encapsulate a large amount of chemo-drugs and extremely hydrophobic PFP (Fig. 1a). Based on the nano-sized particle structure, we expected that Echo-CNPs with both anticancer drug

and PFP could be localized at targeted tumors through the enhanced permeability and retention (EPR) effect. In contrast, microbubbles are not allowed to extravasate from the blood vessel to the surrounding tissues due to their micro-sized dimensions (Fig. 1b). Moreover, we hypothesized that the echogenic Echo-CNPs can visualize and cure the target tumor tissue simultaneously via cancer-targeted, US-triggered imaging and drug delivery. Echogenic Echo-CNPs can improve the drug release profile by external US irradiation, resulting in a burst release of the anticancer drugs at targeted tumor tissues. Therefore, the promising theranostic aspect of Echo-CNPs can impact cancer-targeted imaging and US-triggered drug delivery, simultaneously.



Passive tumor targeting by EPR & US-triggered drug dumping at tumor site

Figure 1. (a) Schematic illustration of echogenic chitosan-based nanoparticles (Echo-CNPs). Glycol chitosan polymer was modified by hydrophobic 5β-cholanic acids, enable it to make self-assembled nanoparticles in the aqueous condition. The chemo-drug was loaded into CNPs when they were self-assembled, and theranostic Echo-CNPs were formulated by emulsification with PFP. (b) Gas bubbling and drug releasing behaviors of PFP/chemo-drug co-loaded Echo-CNPs, and passive tumor targeting by EPR and US triggered drug delivery process.

In order to develop theranostic Echo-CNPs, first, each glycol chitosan polymer was chemically modified with 158 ± 5.6 molecules of hydrophobic 5β -cholanic acid. This provides the hydrophobic driving force to assemble glycol chitosan nanoparticles (CNPs) spontaneously, possessing hydrophobic inner cores of 5β -cholanic acid in the aqueous condition.[27-30] Secondly, anticancer drugs, docetaxel (DTX) or doxorubicin (DOX) in methylene chloride solution was added dropwise followed by a simple dialysis process to formulate DTX-encapsulated CNPs (DTX-CNPs) or DOX-encapsulated CNPs (DOX-CNPs). Drug-encapsulated CNPs formed a stable nanoparticle structure with an average diameter of 300 nm, and the drug-loading efficiency was approximately 90%. Finally, to make echogenic CNPs using the oil in water (O/W) emulsion method, an oil-phased PFP solution (1%, v/v) was slowly mixed with the pre-formulated DTX-CNPs or DOX-CNPs and both NPs were emulsified again in an ice bath to

construct drug- and PFP-encapsulated CNPs (Echo-CNPs). As a control, native glycol chitosan polymer without 5β -cholanic acid moieties-PFP mixture (PFP-GC) and commercially available lipid-based microbubbles, Sonovue®, were tested together as micro-sized echogenic particles.

Physicochemical Properties of Theranostic Echo-CNPs

Size distributions of Echo-CNPs in saline at 25°C were observed by dynamic light scattering (DLS), compared to control particles, PFP-GC and Sonovue® (Fig. 2a). As expected, the self-assembled DTX-CNPs with 10 wt% of DTX had an average diameter of 287 ± 25 nm with a narrow size distribution. After loading PFPs into DTX-CNPs, the echogenic Echo-CNPs still appeared homogeneous and showed *in vivo*-favorable nano-size distribution although their average size was increased up to 432 ± 32 nm.

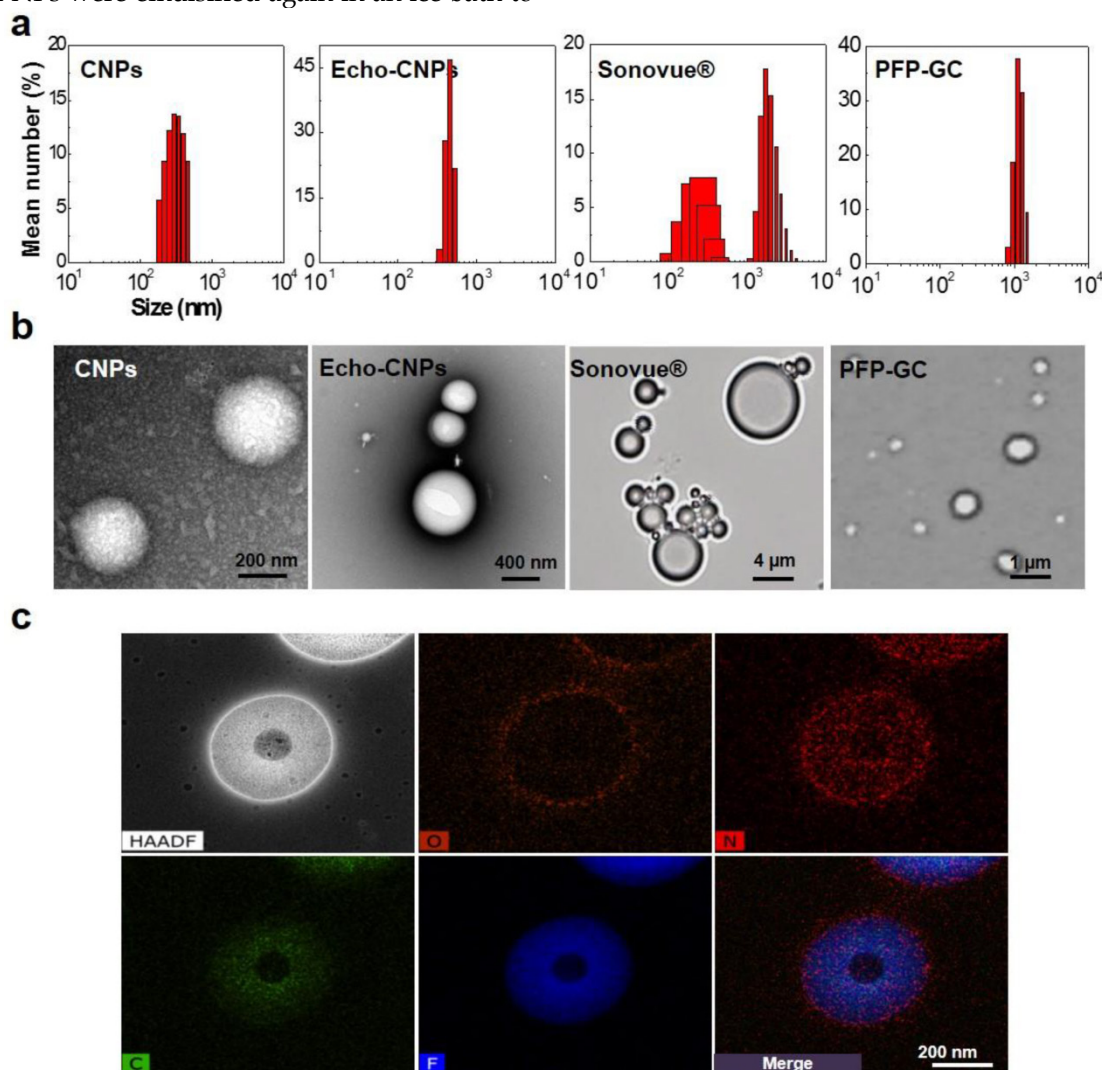


Figure 2. Physico-chemical properties of Echo-CNPs. (a) Hydrodynamic size distribution of CNPs, Echo-CNPs, Sonovue® and PFP-GC in distilled water at 25 °C (b) TEM images of CNPs and Echo-CNPs, and optical images of Sonovue® and PFP-GC (c) Chemical compositions and distributions in the Echo-CNPs analyzed by TEM-EDX. Blue colored PFP was evenly distributed inside the CNP scaffold. O presents hydroxyl group, N presents amine and F presents fluorine.

The commercialized Sonovue® microbubbles and a simple mixture of PFP and GC showed heterogeneous size distributions with average diameters of 2889 ± 465 nm and 1241 ± 123 nm, respectively. The precise nanostructure of Echo-CNPs was also confirmed using TEM after the negative staining of glycol chitosan polymers with uranyl acetate to enhance the contrast between the drug/PFP region and the stainable glycol chitosan polymer regions. As a result, spherical nanoshapes were clearly observed (Fig. 2b) but no noticeable differences were found between the before and the after PFP encapsulation into CNPs at 25 °C. In optical microscopic images, one of the controls, native GC polymer without hydrophobic 5 β -cholanic acids, showed micro-sized particle structure after loading PFP at 25 °C in the buffered condition. Meanwhile, conventional Sonovue® microbubbles composed of sulfur hexafluoride gas inner cores and lipid shell layers also presented micro-sized bodies. Moreover, the unstable outermost lipid shell layers of Sonovue couldn't withstand the evaporating sulfur hexafluoride gas that the size of the microbubbles became bigger even at room temperature. These comparative observations clearly implied that the hydrophobic driving force that existed on the chemically modified GC polymer was a decisive factor to load PFP inside CNPs and to maintain their small and robust nanostructure.

In order to predict the nanostructure of PFP-loaded Echo-CNPs more precisely, the chemical compositions of Echo-CNPs were analyzed by TEM-EDX (Fig. 2c). From Fig. 2C, O (orange), which represents the hydroxyl group of GC polymers, was observed in the outermost surface layer of particles, which means Echo-CNPs were surrounded by hydrophilic hydroxyl parts of GC polymers. As expected, N (red), which represents the amine group of GC polymers, was distributed in the entire particle, indicating that Echo-CNPs were mainly comprised of GC polymers. For F (blue), which represents the fluorine of PFP, it was evenly distributed inside the GC polymer scaffolds of the nanoparticles. Since PFPs are encapsulated into the hydrophobic pocket of CNPs when they are self-assembled, as discussed before, this result is well correlated with the previous results.

Temperature-Dependent Bubble Formation Process of Echo-CNPs

In order to predict the bubble formation process and the *in vivo* behaviors of Echo-CNPs, the time-dependent size variations were observed and measured by optical microscopy and DLS, respectively. As results, Echo-CNPs did not show a noticeable size increase in saline during the first 20 min incubation at 25°C, while large micro-sized bubbles

were clearly observed in the optical microscopic images after 20 min post-incubation in the same buffer at 37°C (Fig. 3a). The DLS measurement showed the accurate size increase tendency over time depending on the external temperature. The size of Echo-CNPs increased quickly from 434 nm to 2 μ m in saline buffer at 37 °C while the size increase rate was slower during the 1 h incubation at 25°C (Fig. 3b). Since the boiling point of PFP is 29 °C, the evaporation of PFP was effectively retarded inside the hydrophobic pocket of Echo-CNPs at room temperature.[26] On the other hand, most of the lipid-based Sonovue® microbubbles disappeared within 20 min even at 25°C. Conventional Sonovue® microbubbles are composed of sulfur hexafluoride gas as inner cores and lipid shell layers. They presented prominent gas-bubbling structures from the nano- to the micro-sized bodies due to the continuous evaporation of the sulfur hexafluoride gas (boiling point; - 63 °C) in the buffered condition at 25 °C. The soft outermost lipid shell layers of Sonovue® couldn't withstand the pressure of the evaporating sulfur hexafluoride gas. The size of the microbubbles increased dramatically even at room temperature. Meanwhile, the other control group, PFP-GC mixture, also showed a fast size increase rate within the 10 min incubation at 25 °C, and finally the GC polymers formed macro-sized aggregates, indicating most of the PFPs came out and evaporated from the simple PFP-GC mixture. This result indicates that without the hydrophobic molecules, GC polymers cannot make stabilized and robust nanostructures, which can entrap PFPs into their inner cores in an aqueous environment. Taken together, the comparative observations clearly implies that the hydrophobic driving force that exists on the GC polymer is a decisive factor that enables the loading of PFP inside CNPs and maintains their small and robust nanostructure.

More precise TEM observations were performed to visualize the bubble formation process of Echo-CNPs as the external temperature increased (Fig. 3c). As the external temperature increased from 4°C to 60°C in the TEM chamber, the sizes of Echo-CNPs gradually increased by the expansion of GC scaffold as the PFP inside evaporates. Interestingly, the illuminated white spots in Echo-CNPs gradually expanded, while the particle sizes increased from 400 nm to 2 μ m as the external temperature increased from 4 °C to 60 °C. At 60 °C, the body of Echo-CNPs was slightly distorted by partial evaporation of PFP gases from the hydrophobic pockets of CNPs. These unique bubbling behaviors can be explained by the robust and unique nanostructure of Echo-CNPs. The extremely hydrophobic PFP, which exists in the hydrophobic 5 β -cholanic acid inner cores,

evaporates from liquid to gas phase thus expands the CNP scaffold slowly and continuously at above its boiling temperature. At the high temperature of 60 °C, PFP gases bursted from the relatively weak areas of the solid CNPs. More interestingly, after 20 min post-incubation at 37°C in the TEM chamber, when Echo-CNPs were exposed by the external US irradiation (10 MHz; mechanical index: 0.235; average power: 0.0676 W/cm²), collapsed and/or flattened and

contorted CNPs were clearly observed in TEM images (Fig. 3d).

Drug Release and Cellular Uptake of Echo-CNPs

As a drug delivery cargo, Echo-CNPs were loaded with 10 wt% and 30 wt% of DTX via the O/W emulsion method, and the DTX-loading efficiencies were approximately 93% and 61.7%, respectively (Fig. 4a).

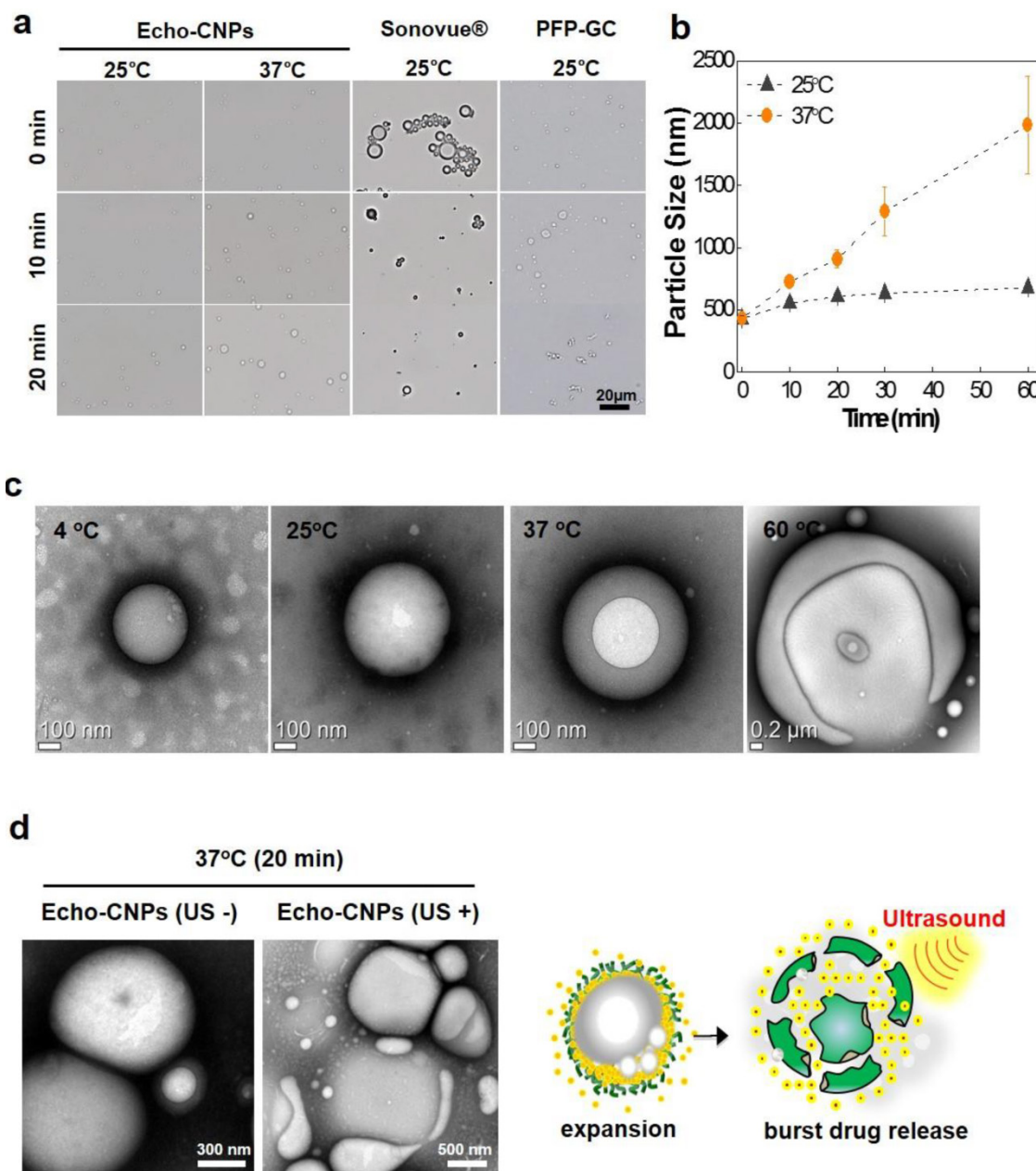


Figure 3. Bubble formation process and behaviors of Echo-CNPs depending on external environments. (a) Evaluation of gas generating behaviors of Echo-CNPs, Sonovue® and PFP-GC over time at 25 °C and 37 °C respectively by optical microscopic image analysis (b) Hydrodynamic size changes of Echo-CNPs in PBS up to 60 min at 25 °C and 37 °C to predict the bubbling formation process and *in vivo* behaviors of Echo-CNPs inside the body over time (c) Morphological changes of Echo-CNPs observed by TEM in order to visualize the bubble formation behaviors depending on the external temperature changes from 4°C to 60°C. (d) The TEM images for visualizing the bubbling Echo-CNPs destruction by exposing to an external US irradiation. Echo-CNPs was incubated in 37 °C PBS during 20 min before destroy mode of US (10 MHz; mechanical index: 0.235; average power: 0.0676 W/cm²) applying.

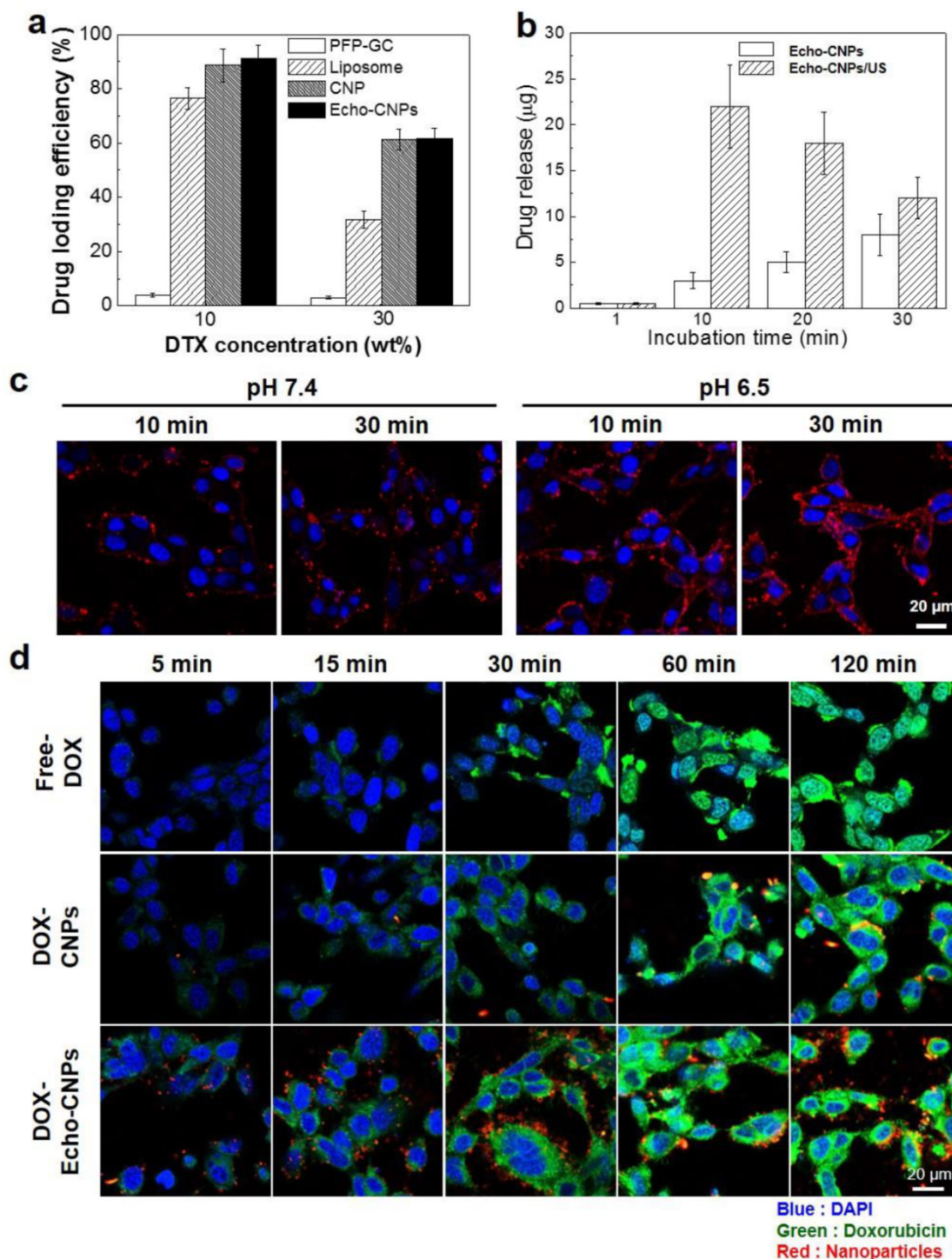


Figure 4. (a) DTX loading efficiency of Echo-CNPs in comparison with liposome, CNPs and PFP-GC at DTX feed ratios of 10 and 30 wt%. (b) US triggered DTX releasing behaviors over time from DTX loaded Echo-CNPs with and without US destrory mode (10 MHz; mechanical index: 0.235; average power: 0.0676 W/cm²) for 5 min to induce bubble destruction (c) pH dependent confocal microscopic images for visualizing cellular uptake of Echo-CNPs at 10 min and 30 min in SCC7 cells. (d) Confocal microscopic analysis of time dependent intracellular DOX localization tendencies of DOX loaded Echo-CNPs with comparison to Free-DOX and non-echogenic DOX-CNPs.

The high drug-loading capacity was comparable to those of liposome and CNPs. However, PFP-GC mixture showed extremely low drug-loading efficiency since GC polymers lack cholanic acid that comprises hydrophobic inner reservoirs to load hydrophobic chemo-drugs. Furthermore, as expected, 10

wt% of DTX-encapsulated Echo-CNPs (DTX-Echo-CNPs) clearly showed US-triggered drug release behaviors via exposure to the external US irradiation (Fig. 4b). When Echo-CNPs were US-irradiated for 5 min at 37°C, 7 times higher amount of DTX was released from Echo-CNPs at 10

min post-incubation, compared to that of Echo-CNPs without the external US irradiation. The high drug-loading capacity and US-triggered drug release behaviors of Echo-CNPs showed that the external US irradiation greatly enhanced the drug release by destroying the PFP gases in Echo-CNPs.

To evaluate the pH-dependent cellular uptake of Echo-CNPs, NIRF Cy5.5-labeled Echo-CNPs (red color) were incubated with SCC7 tumor cells and their intracellular uptake was confirmed by confocal microscopy (**Fig 4c**). Before this cellular uptake test, the cell viability of Echo-CNPs in SCC-7 tumor cell was measured using MTT assay. After 24 h post-incubation, Echo-CNPs (1 mg/ml) did not present any cototoxicity (**Supplementary Fig. 1**). At the normal pH of 7.4, after 10 min incubation, the red fluorescent Echo-CNPs were mainly observed on the outer cellular membrane of SCC7 cells and not in the nucleus (DAPI-stained blue color). At 30 min post-incubation, some of the Echo-CNPs were observed in the cytosol, which indicates cellular uptake of Echo-CNPs, but still the majority of red fluorescence was localized on the outer cellular membrane. On the contrary, at an acidic pH of 6.5, which is the same as the tumoral pH, much stronger red fluorescent signals of Echo-CNPs were observed on the cellular membrane and in the cytosol after 10 min incubation, indicating the enhanced cellular association and internalization of Echo-CNPs at the lower pH. The accelerated cellular uptake of Echo-CNPs at an acidic pH can be justified by the pKa value of amine groups that exist in the GC polymer. The amine groups of GC become protonated and positively charged at a slightly acidic pH, and the positively charged glycol chitosan shell of Echo-CNPs results in the faster binding and cellular uptake of Echo-CNPs by the targeted tumor cells.[30] This finding suggests that the uptake of Echo-CNPs can be greatly enhanced in a tumoral acidic environment, as compared to the normal tissues.

In order to confirm the drug release and the localization tendency inside the cells, fluorescent doxorubicin (DOX) was used as a model drug instead of DTX. The intracellular fate of physically encapsulated DOX molecules in Echo-CNPs was monitored in the SCC7 tumor cells over time (**Fig. 4d**). In the case of free DOX, after 1 h incubation, the majority of free DOX (green color) was localized in the nuclei (blue color) at the site of drug action, indicating the rapid drug uptake and the appropriate transfer of the free DOX molecules inside the cells. However, DOX molecules from non-echogenic CNPs were mainly observed in the cytoplasm up to 1 h post-incubation. The result indicates that the release of DOX from non-echogenic CNPs was not effective in the live cells,

due to the slow release and/or endosome entrapment of the physically encapsulated DOX in the CNPs. On the contrary, the rapidly released DOX from Echo-CNPs was mainly localized in the cytosol at the initial time point (10-30 min post-incubation), and then many of the released DOX were observed in the nuclei inside the tumor cells after 1 h incubation. These results imply that expanding Echo-CNPs with PFP evaporation can accelerate DOX release, and the released DOX get effectively transferred to the nucleus, which is the site of drug action.

Furthermore, in order to predict the effect of external US irradiation on the drug release and localization tendency on a cellular level, SCC7 cells were observed by confocal microscopy after the external US irradiation (US Power 100%; 10 MHz; mechanical index: 0.235; average power: 0.0676 W/cm²) into the Echo-CNPs-treated cells and non-treated cells. Importantly, the external US irradiation for *in vitro* tests did not present any toxicity to the control and Echo-CNP-treated SCC7 cells after 5 min US-irradiation (**Supplementary Fig. 2**). As a result, after 30 min incubation, the external US irradiation promoted the drug release (green color) from Echo-CNPs (red color) by interacting with the echogenic Echo-CNPs (**Fig. 5a**). Interestingly, it was evident that the interaction of US and Echo-CNPs induced the desired movement of the released DOX from the cytoplasm to the nucleus (blue color) when the DOX localization was precisely observed 3-dimensionally (**Fig. 5b**). Also, the strong US irradiation may induce the cavitation effect of Echo-CNPs by the expansion, collapse and oscillation of inner PFP bubbles, which can enhance the internalization of therapeutic drugs/genes into targeted cancer cells.[8, 31, 32]

In Vitro Echogenicity and In Vivo US Imaging of Echo-CNPs

The echogenic properties of Echo-CNPs were investigated in agar-gel phantom in comparison to those of PFP-GC and Sonovue® as control echogenic particles. When the weight ratio of PFP to Echo-CNPs was increased from 0.5 wt% to 5 wt% in saline at the body temperature of 37 °C, the US intensity was proportionally increased and saturated at 5 wt% (**Fig. 6a and 6b**). We also tested the dose-dependent echogenic properties of Echo-CNPs containing 5 w% of PFP in order to verify that Echo-CNPs can generate strong US signal even in biologically relevant highly diluted condition ranging from 0.1 to 1 mg/ml of Echo-CNPs concentration in the same agar gel phantom condition. When the biologically relevant dose-dependent US intensities of Echo-CNPs were acquired after 1 h post-incubation (**Supplementary**

Fig. 3), Echo-CNPs presented the strong US intensity at the more diluted concentration of PFP and CNPs that can be available for *in vivo* US imaging. Moreover, as expected, the strong US signals of Echo-CNPs persisted for 120 min, and the half-life of echogenicity was 49 min (Fig. 6c and 6d). The duration of the echo signals of Echo-CNPs was approximately 5 times longer than that of commercially available Sonovue® and GC-PFP, 9.2 min and 10 min, respectively, in the same condition (Fig. 6d). As described above, since the stabilized and robust CNP scaffold can detain the vaporization of the encapsulated PFP, the duration and the intensity of the US signals well correlated with the size variations, and were also dependent on the external temperature and the incubation time.

The *in vivo* tumor-targeted US imaging ability of Echo-CNPs was also confirmed by intravenous (i.v.) injection of Echo-CNPs into SCC 7 tumor-bearing mice. When the tumor sizes reached 150 mm³, Echo-CNPs (16 mg/kg) or Sonovue® (40 mg/kg) was injected and the US intensity at the tumor tissue was observed (Fig 6e). As a result, within 1 min post-injection, the bright and strong echo signals

began to be observed via US imaging, indicating effective tumor accumulation of Echo-CNPs. More importantly, the strong US signals persisted for 1h at the tumor site, which can be attributed to the continuous PFP gas generation inside Echo-CNPs at the targeted tumor tissue. In contrast, the US signal of Sonovue® in the target solid tumor was not enough to visualize the whole tumor, which means inefficient amount of micro-sized Sonovue® was accumulated in the tumor after the i.v. injection. It is well known that the easily vaporizable, thus diffusible sulfur hexafluoride gas of Sonovue® in the blood is not stable in the US field, so they disappear within 5 min inside the body.[33] Also, Sonovue® would not be able to circulate the whole body repeatedly due to its micro-sized dimension. However, outstanding physico-chemical properties of echogenic Echo-CNPs as an ultrasound contrast agent as well as a drug delivery cargo resulted in prominently improved US tumor imaging. Moreover, the high quality of US imaging of tumor can be rationalized by the following *in vivo* whole body distribution and the tumor accumulation of Echo-CNPs.

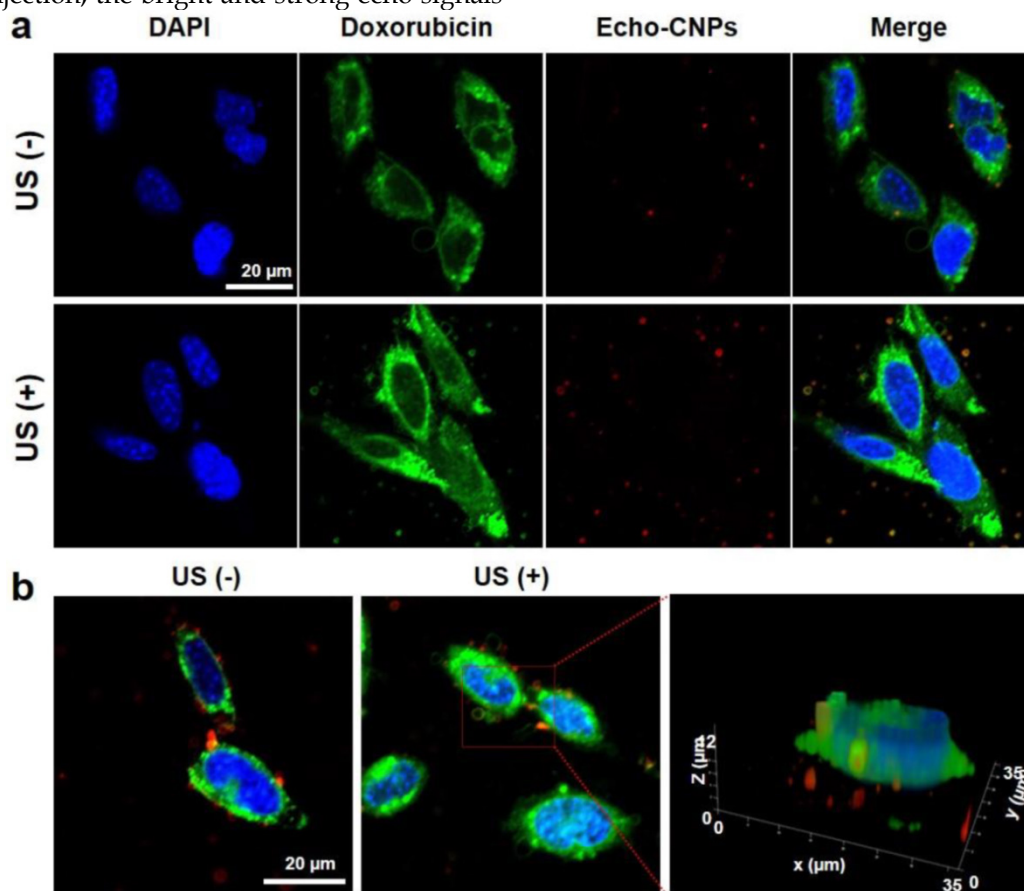


Figure 5. The effect of external US irradiation on the drug release and localization tendency on a cellular level. The DOX-encapsulated Echo-CNPs (10 μg/ml of DOX) were incubated in SCC7 cells for 30 min and the external US irradiation (10 MHz; mechanical index: 0.235; average power: 0.0676 W/cm²) was applied to each cell directly for 5 min. After 30 min post-incubation, the cells (blue color for nuclei) were washed with PBS and then the cells were fixed and imaged with confocal laser microscope. (a) US triggered intracellular DOX (green color) release from Echo-CNPs (red color) without/with the external US irradiation. (b) Precise 3-Dimensional observation of released DOX molecules inside SCC7 cells after the external US irradiation. The quantification and 3-D modeling of DOX-encapsulated Echo-CNPs was analyzed by Leica software.

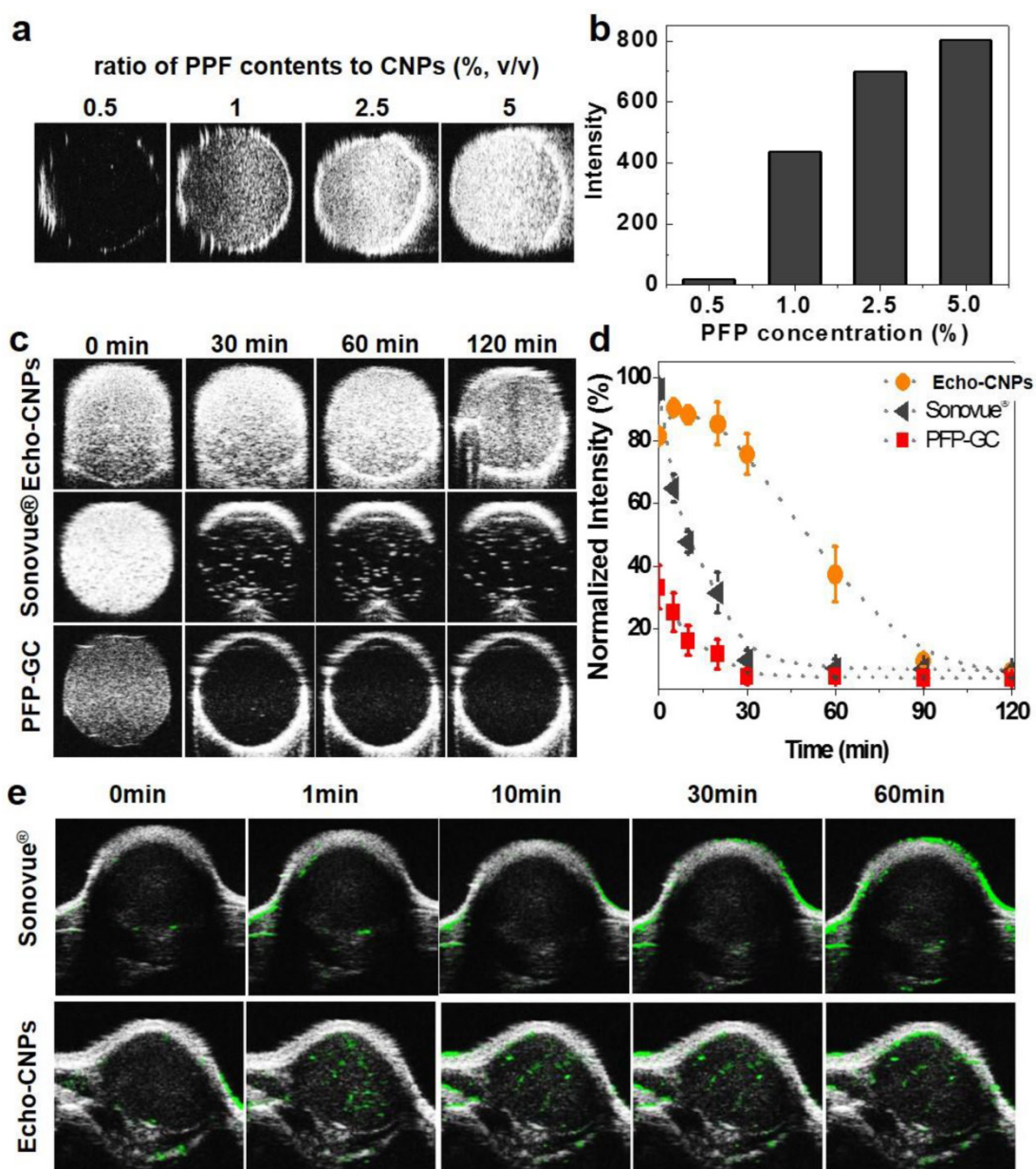


Figure 6. Echogenic properties of Echo-CNPs *in vitro* and *in vivo*. (a) US signals generated by Echo-CNPs with varying PFP contents (0.5–5 %, wt) at 37°C. US signals were visualized under agar phantom gel as 40 MHz of US was applied. (b) Normalized US intensities of Echo-CNPs at different PFP concentrations (c) Time dependent US intensities in agar phantom gel of Echo-CNPs compared to those of Sonovue® and PFP-GC in the same experiment condition (d) Normalized time dependent US intensities of Echo-CNPs, Sonovue® and PFP-GC. (e) *In vivo* US imaging ability of Echo-CNPs compared to a conventionally available Sonovue®. After tail vein injection of Echo-CNPs into SCC7 tumor bearing mice, the US signals from solid tumors were acquired over time from 0 to 60 min by applying of 40 MHz US with contrast mode of Vevo 770®.

In vivo Biodistribution of Echo-CNPs in Tumor-Bearing Mice

To confirm the tumor-targeting efficiency of Echo-CNPs with and without any direct exposure to an external US, Flamma™-labeled and 10wt% DTX-encapsulated Echo-CNPs were non-invasively imaged in SCC7 tumor-bearing mice. When the tumor size reached approximately 150 mm³, 5 mg/kg of Echo-CNPs were intravenously administered through the tail-vein injection. To evaluate the enhanced tu-

mor targeting ability by the generation of acoustic cavitation through the interaction of echogenic Echo-CNPs with US, US was applied to the solid tumors directly for 10 min, after 3 min post-injection. We hypothesized that US and oscillating echogenic Echo-CNPs can generate a biologically useful energy to enhance the permeability of the surrounding vessels to allow deep tumor tissue penetration of the nanoparticles.[31]

At 1 h post-injection, dorsal tumor tissue was clearly delineated from the surrounding normal tissue

in both groups of with and without US, demonstrating the tumor-specific targeting ability of Echo-CNPs. Non-invasive NIRF images revealed that the Echo-CNPs gradually accumulated for up to 2 days post-injection, due to the EPR effect, facilitated by the *in vivo*-favorable size of Echo-CNPs (Fig. 7a). Interestingly, in the US treated group, the tumor accumulation of Echo-CNPs was more prominent and faster than the US non-treated group in the whole body distribution images up to 2 days. Specifically, the maximal difference in tumor accumulation of

Echo-CNPs between the US-treated and non-treated groups was observed at 3 h post-injection. US-treated group showed 4-7 times higher tumor accumulation based on the measurements of the fluorescent intensities of the excised tumors (Fig. 7b). US-treated group showed even wider distribution of Echo-CNPs inside the excised tumor compared to the non-treated group (Fig. 7c), indicating that Echo-CNPs could penetrate the main vessels to reach the surrounding tumor tissue effectively by generating acoustic cavitation from echogenic Echo-CNP-US interaction.

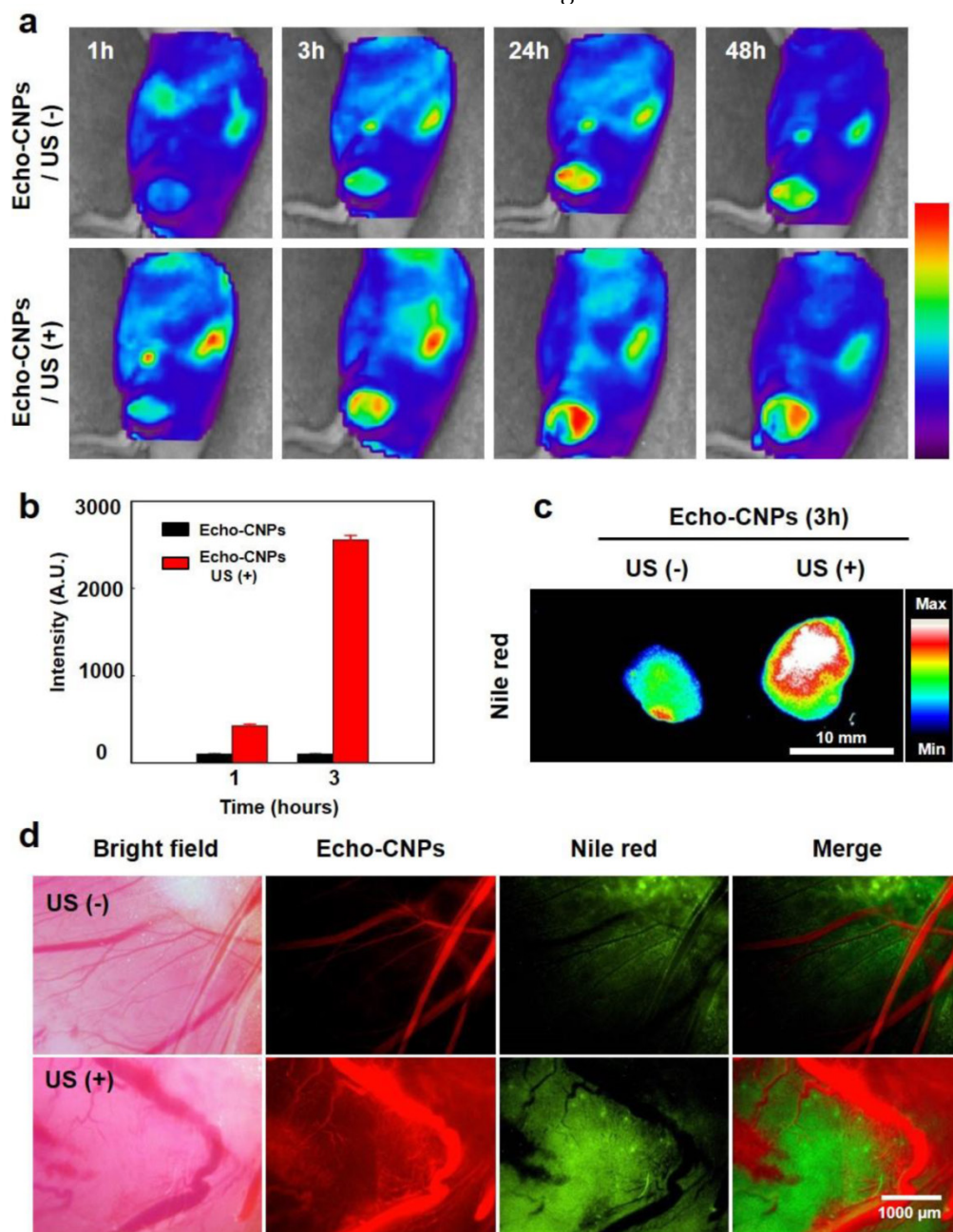


Figure 7. (a) Biodistribution of fluorescent Flamma™ labeled Echo-CNPs after *i.v.* injection with or without US irradiation (10 MHz; mechanical index: 0.235; average power: 0.0676 W/cm²) was analyzed with eXplore Optix system. After a 3 min post-tail vein injection, US was applied into the solid tumor directly during 5 min with US destruction mode to induce destruction of the gaseous PFP inside Echo-CNPs (b) Normalized fluorescent intensities at tumor tissue after 1 h and 3 h post-injection and followed by US treatment during 5 min (c) *ex vivo* fluorescent imaging of the excised tumor tissues (d) Direct visualization of real-time model drug release behaviors by OV-100 micro-vessel imaging system at the target tumor tissue after 10 min tail vein injection. The targeted tumor region was exposed to an external US destruction mode for 5 min.

To predict and visualize the US-triggered drug release in *in vivo* condition more clearly, 10 wt% of fluorescein Nile red-encapsulated Echo-CNPs (100 μ L in saline, 10 mg/kg of Nile red) were intravenously injected, when the tumor sizes became approximately 150 mm³ in volume in SCC7 tumor-bearing mice. The fluorescent Nile red released from the Echo-CNPs in tumoral vessels was visualized using OV 100 micro-vessel imaging system. After 10 min post-injection, the targeted tumor region was treated with US for 5 min on the US destruction mode (10 MHz; mechanical index: 0.235; average power: 0.0676 W/cm²) to induce the destruction of the gaseous PFP of the Echo-CNPs (Fig. 7d). As a result, prominent and a wide range of Nile red fluorescence distribution was observed in the entire tumor tissue with the US treatment, while faint and narrow distribution of Nile red was resulted in the US non-treated group. Those comparative images with and without US clearly showed that the use of echogenic Echo-CNPs with US could greatly improve the drug delivery efficiency in terms of US-triggered drug release as well as cavitation-induced enhancement of the vessel permeability.

Therapeutic Efficacy of Echo-CNPs in Tumor-bearing Mice

To evaluate the therapeutic efficacy of Echo-CNPs, 10 wt% of DTX-encapsulated Echo-CNPs were administered to SCC7 tumor-bearing mice (n=5), and the tumor growths were monitored for 15 days. In brief, when the tumors were grown to 15-20 mm³, four different types of treatments: injection of (1) saline, (2) free DTX (10 mg/kg) (3) DTX-encapsulated Echo-CNPs (10 mg/kg DTX), and (4) DTX-encapsulated Echo-CNPs (10 mg/kg DTX) followed by US irradiation (n=5), were conducted for the tumor therapy once every three days for 12 days. For the US irradiation, the destruction mode of US (10 MHz; mechanical index: 0.235; average power: 0.0676 W/cm²) was applied to the tumor sites after 10 min, 30 min and 1 h post-injection of Echo-CNPs.

First, the therapeutic efficacy of each sample was examined by measuring the tumor volumes over the course of 15 days (Fig. 8a and 8b). As expected, the control saline group did not present any therapeutic efficacy and the mean tumor volume changed from 15 mm³ to 1,843 mm³. On the 15th day, however, DTX-encapsulated Echo-CNPs -treated mice presented a dramatic reduction in the tumor volume when a series of ultrasound irradiation was applied; the final mean tumor volume was 16 ± 1.2 mm³ by the end of the study (mean \pm s.e., n=5, ANOVA at 95% confidence interval), which is significantly smaller than that of the free DTX-treated mice (840 mm³) (Fig. 8b). Furthermore, in comparison with the DTX loaded

Echo-CNPs -treated mice, after US irradiation, DTX-encapsulated Echo-CNPs -treated mice showed the smallest tumor size, which is 0.8 % of free DTX-treated group, indicating that the enhanced therapeutic efficacy of Echo-CNPs can be achieved by the US-triggered drug release at the target tumor tissue. In the histological analysis, H&E staining clearly showed a substantial damage inside the tumor tissue in the US-treated, DTX-encapsulated Echo-CNPs group (Fig. 8c). From the therapeutic efficacy data, the US-irradiated Echo-CNPs might have increased the local concentration of the released drug in the target tumor, resulting in the maximized anti-tumor therapeutic efficacy. [21,27]

Conclusions

The outstanding physico-chemical properties and the sophisticated nanostructure of the hydrophobic core-hydrophilic shell layer of Echo-CNPs highlight two advantages as US-responsive multimodal theranostic nanoparticles. First, the inner hydrophobic cores of Echo-CNPs can function as a robust and effective reservoir for both chemo-drugs and PFPs. The function as a gas container is noteworthy in terms of the effective retardation of the gas expansion and the maintenance of the physical and mechanical stability. This aspect results in the prolonged half-life of Echo-CNPs in the bloodstream that they remain in the circulation long enough to reach the target site *in vivo*, benefited from the *in vivo*-friendly nanoscale size. Second, hydrophilic GC polymers of the outermost shell layer provide excellent *in vivo*-friendly physico-chemical properties such as serum stability and biodegradability as well as tumor-homing ability. The newly developed Echo-CNPs could be utilized as drug delivery vehicles as well as ultrasound contrast enhancers, which could achieve site- and time-specific drug release by externally applying US for cancer treatment.

Experimental Section

Materials. Glycol chitosan (Mw=250 kDa; degree of deacetylation=82.7%), 5 β -cholic acid, N-hydroxysuccinimide (NHS), 1-ethyl-3-(3-dimethylaminopropyl)-carbodiimide hydrochloride (EDC), dichloromethane (DCM) were purchased from Sigma Chemical Co. (St. Louis, MO). Perfluoropentane (PFP) 99% was obtained from Apollo Scientific Ltd.(Manchester, UK) and Sonovue® was purchased from Bracco Diagnostics, Inc. (Milan, Italy). As anti-cancer drugs, docetaxel (DTX) and doxorubicin HCl (DOX) were purchased from Sigma Chemical Co. (St. Louis, MO). For fluorescence imaging, Nile-red was obtained from Sigma Chemical Co. (St. Louis, MO) and Flamma™ (FPR-675) was purchased from Bioacts

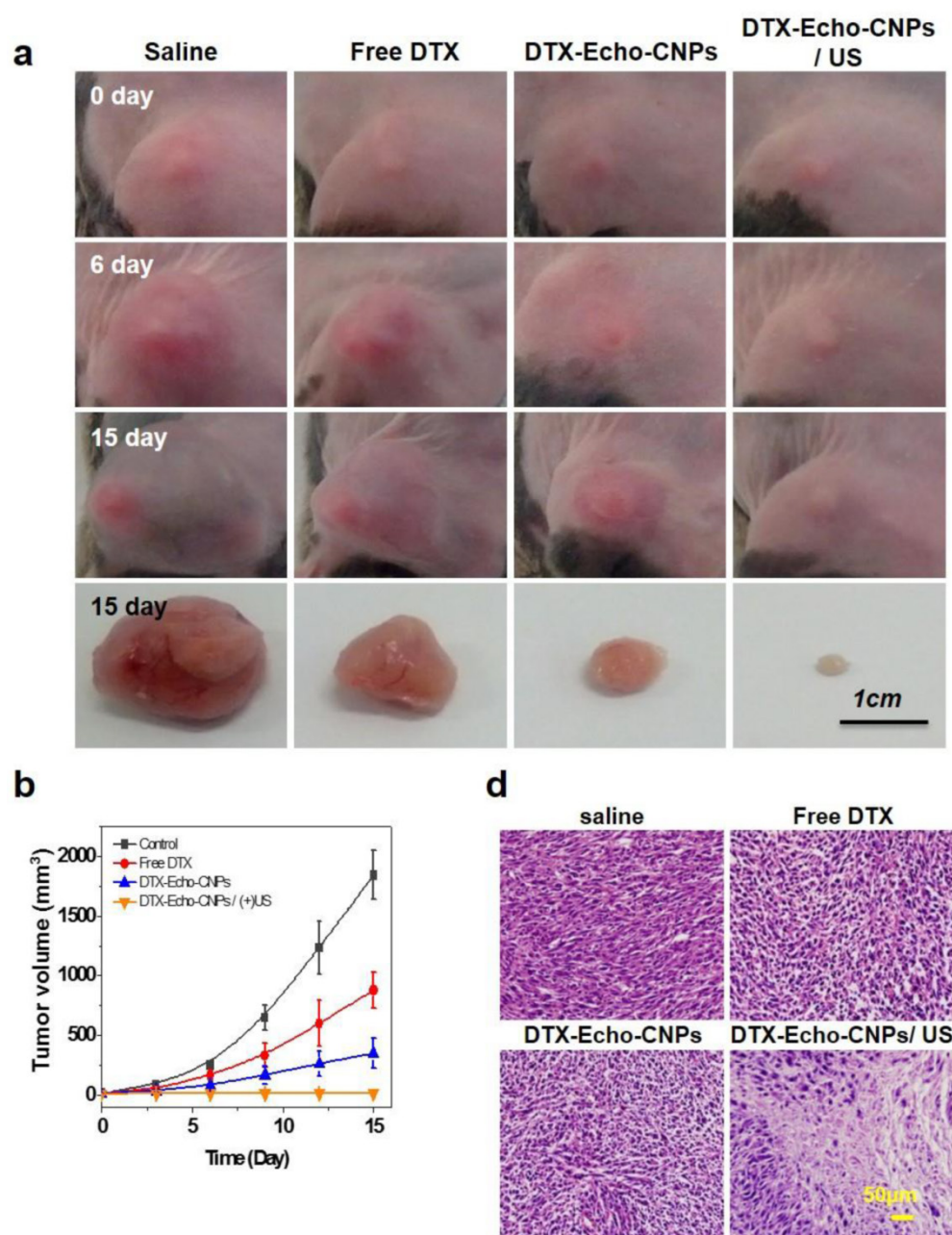


Figure 8. Therapeutic efficacy of Echo-CNPs with combination of external US irradiation. (a and b) Antitumor therapeutic efficacy of DTX loaded Echo-CNPs by measuring tumor volumes over 15 days. DTX- Echo-CNPs were administered into each experiment group per 3 days, and US destruction (10 MHz; mechanical index: 0.235; average power: 0.0676 W/cm²) was conducted after a 3 min injection of DTX-Echo-CNPs. (c) Histological changes of tumor tissues by hematoxylin-eosin (H&E) staining.

(Incheon, Korea). Dimethylsulfoxide (DMSO) and methanol (MeOH) were used reagent grade without further purification. Squamous cell carcinoma (SCC7) was purchased from the American Type Culture Collection (ATCC, Rockville, MD, USA). For cell culture, RPMI-1640, trypsin-EDTA and fetal bovine serum (FBS) were purchased from Welgene Inc (Daegu, Korea).

Preparation of DTX-loaded CNPs (DTX-CNPs). Hydrophobically modified glycol chitosan (HGC) was

prepared by following the previous report [27, 34]. In brief, HGC was synthesized by chemical conjugation between glycol chitosan (GC) and 5 β -cholanic acid (CA) in the presence of EDC and NHS. After dissolving GC and CA into distilled water (DW) and MeOH respectively, EDC and NHS were added into CA solution to activate the carboxyl group of CA to react with the amine group of the GC polymer. Then, GC solution was slowly added into CA solution with vigorous stirring and the mixture was incubated for

24 hrs at room temperature. After the reaction, it was dialyzed against MeOH/DW mixture and DW for 3 days, and lyophilized. Final chitosan nanoparticles (CNPs) were prepared by self-assembly of HGC in aqueous solution. For particle preparation, 2 mg of HGC was dissolved in DW (1 mL) and sonication was conducted for 5 min, using a probe-type sonicator (Ultrasonic processor 750W, Cole-Palmer, IL, USA). As an anticancer drug, docetaxel (DTX) was loaded into CNP using emulsification method. For drug incorporation, 3 mg of DTX was dissolved in DCM (0.6 mL), and it was dropped into CNP solution (27 mg/ 6 mL) undergoing sonication. Then, the emulsion was concentrated for 3 hr to remove residual DCM, and 30 mL of DW was added with stirring. After 30 min, it was dialyzed against DW for 2 days, and lyophilized. To compare the drug-loading efficiency of CNPs with raw glycol chitosan polymer (native GC) and liposome carrier, DTX was also formulated into both polymers. DTX-loaded native GC particles were prepared using the same method for DTX-CNPs, and DTX-loaded liposomes were prepared through the solvent evaporation method using phosphorylcholine lipid. 10-30 % (w/w) of DTX was formulated into CNP, native GC, and liposome, and drug-loading efficiency was measured by high performance liquid chromatography (HPLC) (Agilent Tech., CA, US) equipped with C18 column.

Preparation of Echogenic Nanoparticles (Echo-CNPs). In order to introduce echogenic property into CNPs, perfluoropentane (PFP), which has a boiling point (bp) of 29 °C was formulated into the CNPs by oil in water (O/W) emulsification method with PFP (oil phase) and HGC polymer (water phase). For preparation of Echo-CNPs, 2 mg of HGC polymer was dissolved in DW (1 mL) and placed in an ice bath with probe type sonicator. Then, PFP (0.5~5 %, v/v to total solution) was slowly added into the polymer solution under a sonication process (25% power, 5 sec On/ 1 sec Off) for 2 min. To compare the echogenic property and the stability of the particles, as a control group, GC-coated PFP particles (GC-PFPs) were also prepared with native GC polymer using the same method for Echo-CNPs. Both Echo-CNPs and GC-PFPs were stored in rubber capped vial at 4 °C and the storage did not exceed 1 hr to prevent vaporization. For anticancer therapy, DTX-loaded Echo-CNPs were prepared with DTX-CNPs. 10-30 % (w/w) of DTX-containing DTX-CNPs were dissolved in 1 mL, and 5 μ L of PFP was added under sonication. The drug-loading contents were measured by HPLC using the same condition.

Characterization of Echo-CNPs. The size distribution of Echo-CNPs, CNPs, GC-PFPs and Sonovue® were measured by zeta-sizer (Malvern

Zetasizer; Malvern Ins.Ltd., UK) with 633 nm wavelength. Each particle system was diluted in DW (10 %, v/v) and the sizes were measured after the incubation at 25 °C for 5 min. The sizes were measured three times and the mean diameter was determined by number means. The morphology of Echo-CNPs, CNPs, PFP-GC and Sonovue® was observed by transition emission microscopy (TEM, CM-200, Philips, CA). For sample preparation, each sample was incubated in DW for 5 min at 25 °C, dropped onto copper grid (400-mesh), and stained with 5% (w/v) of uranyl acetate solution. To evaluate the size changes of Echo-CNPs depending on the time at practical condition, the sizes were measured for 60 min at 25 °C and 37 °C, and their sizes were simultaneously visualized by optical microscope (BX51; Olympus Co. Ltd., Japan) attached with a 40x focal lens. The morphological changes of Echo-CNPs at different temperatures (4 °C ~ 60 °C) were also observed by TEM. For observation, Echo-CNPs were incubated at different temperature for 5 min and stained by uranyl acetate solution using the same process above. The size, shape, and element mapping analysis of Echo-CNPs were observed by transmission electron microscopy at 200kV (Talos™ F200X, FEI Corporate, Oregon, USA). The chemical compositions of Echo-CNPs were determined by the energy dispersive x-ray spectroscopy (EDS) with 4-channel detector (Talos™ F200X, FEI Corporate, Oregon, USA), and mapping analysis of elements was performed based on the differential phase contrast (DPC) information using Velox™ S/TEM software (FEI Corporate, Oregon, USA).

In vitro Release of DTX loaded Echo-CNPs. In vitro drug release profile of DTX-loaded Echo-CNPs was determined by HPLC after sinking in the PBS/tween 80 mixtures (20mL). In brief, DTX-loaded Echo-CNPs (10%, w/w) were dispersed in PBS (5 mg/mL) and placed into a dialysis membrane (MWCO = 6,000~8,000). The dialysis membrane was sunken in 20 ml of PBS/tween80 (99.9/0.1) solution at 37 °C. The sinking buffer was sampled periodically up to 48 h and fresh medium was refilled every time. Release profile of DTX from Echo-CNPs was analyzed using HPLC equipped with C18 column at 40 °C. In order to evaluate the drug release by US irradiation, the destruction mode of US (US 100% power; 10 MHz; mechanical index: 0.235; average power: 0.0676 W/cm²) was applied to the DTX-encapsulated Echo-CNPs and their release amounts were compared with non-US Echo-CNPs. For US irradiation, DTX-Echo-CNP containing dialysis membrane was laid in a hand-made tool filled with PBS/tween solution (20 mL) and the destruction mode of US was applied to the DTX-encapsulated Echo-CNPs for 5 min using Vevo770® system. The sinking buffer was

sampled and analyzed as mentioned above.

In vitro Cellular Uptake and Release Behavior of DOX. In order to determine cellular uptake behavior of Echo-CNPs, flamma™ was labeled to CNPs and Echo-CNPs were prepared with PFP. For *in vitro* cell uptake, SCC7 cells (1×10^5 cells/well) were seeded onto glass bottom dish (35 mm), and 100 $\mu\text{g}/\text{ml}$ of Echo-CNPs solution was added into the cells at different pH conditions (pH 6.5 and 7.4). After 10 and 30 min post-incubation, the cells were washed with PBS, and fixed with 4 % of formaldehyde solution for imaging. To demonstrate the drug release behavior of Echo-CNPs, DOX was encapsulated into the Flamma™-labeled CNPs and Echo-CNPs were prepared with PFP (1 % v/v). After seeding SCC7 cells (1×10^5 cells/well) onto dish (35 mm), free DOX, DOX-encapsulated CNPs (DOX-CNPs) and DOX-encapsulated Echo-CNPs (DOX- Echo-CNPs) (10 $\mu\text{g}/\text{ml}$ of DOX) were added to the cells, and incubated for specific amounts of time. Then the cells were washed and fixed. To verify the US-triggered drug release behavior of Echo-CNPs, DOX- Echo-CNPs (10 $\mu\text{g}/\text{ml}$ of DOX) was treated onto SCC7 cells (1×10^5 cells/well), and after 30 mins of incubation, the destruction mode of US (10 MHz; mechanical index: 0.235; average power: $0.0676 \text{ W}/\text{cm}^2$) was applied directly to the cells for 5 min. After washing with PBS, the cells were fixed for imaging. All *in vitro* cellular images were obtained by confocal laser microscope (Leica TCS SP8, Leica Microsystems GmbH, Germany) with 405 diode (405 nm), Ar (458, 488, 514 nm) and He-Ne (633nm) lasers. The quantification and 3-D modeling was analyzed by Leica software.

Cytotoxicity of Echo-CNPs. Cell viability of Echo-CNPs was confirmed by 3-(4,5-Dimethylthiazol-2-yl)-2,5-diphenyl tetrazolium bromide (MTT) assay. SCC-7 cells were maintained in RPMI 1640 (containing 1% antibiotics and 10% of fetal bovine serum) and seeded onto 96-well tissue culture plate (1×10^4 cells/well). After incubation, 200 μL of Echo-CNPs diluted with cell culture medium (1 μg ~10 mg/mL) were added to each well. The cells were further incubated at 37°C for 24 h. Cells were stained with MTT solution for 2 h and then absorbance was measured by Microplate reader (VERSAmatrix™, Molecular Devices Corp., Sunnyvale, CA). Cell viability was calculated with the ratio between the normal cells to Echo-CNPs treated cells. Also, the cell viability of CNPs and Echo-CNPs with US treatment was determined using live and dead assay following the previous report. In brief, SCC7 cells (1×10^5 cell/well) were seeded in glass bottom dish (35 mm) and 2 ml of CNPs and Echo-CNPs (1 % v/v of PFP) were added into each dish. The cells were directly exposed to US and washed with PBS. After adding staining solution

into each dish, fluorescent images were obtained using IX81-ZDC focus drift compensating microscope (Olympus, Tokyo, Japan).

Ultrasound Imaging In vitro. All the US images *in vitro* and *in vivo* were obtained by Vevo770® (High-Resolution Micro-Imaging System, Visualsonics, Toronto, Canada) equipped with RMV 706 probe at 40 MHz. For *in vitro* experiments, agar-gel phantom was made by molding ependorf tube (500 μL) in agar-gel to mimic conditions similar to our body. [20] Then, 300 μL of each sample was administered into the agar-phantom and the round shaped US images were obtained at contrast mode of Vevo770® software. In brief, various PFP concentrations (0.5~5.0 %) of Echo-CNPs were incubated in agar-gel phantom for 1 min with heating pad (37 °C) and images were obtained. In order to compare the time-dependent US signal of Echo-CNPs to Sonovue® and PFP-GC, each sample (5%, v/v of PFP) was administered in agar-gel phantom for specific amounts of time. The normalized US intensities were calculated by subtracted ROI ratios between water control and sample's intensity.

Ultrasound Imaging of Tumor-bearing Mice. All animal studies were performed within the relevant laws and guidelines of Korea Institute of Science and Technology (KIST) and institutional committees. For *in vivo* US imaging, the tumor model was established using subcutaneous injection of SCC-7 cells (1×10^6) into 5.5 week-old C3H/HeN male mice (n=3, 25-30 g) at the lower back site. When the tumors grew to approximately 100~150 mm^3 , mice were anesthetized using isoflurane gas fixed in an animal pad (Vevo770® maintained at 37°C) and mice hair was removed with depilatory cream for imaging. After covering with aqua-gel (US-gel) on tumor, ultrasound probe (RMV 706) was located on the center of the tumor surface. Before the injection, pre-injection image was obtained, and 200 μL of Echo-CNPs was intravenously injected using a catheter syringe. Then, US images of tumor tissue were observed for 60 min at 40 MHz with contrast mode of Vevo 770® software. In order to compare the US enhancing ability of Sonovue® to Echo-CNPs at tumor site, 200 μL of Sonovue® was also injected and tumor tissue was imaged using the same procedure. The obtained US intensity was normalized by ROI ratio between the background (aqua-gel) and the tumor intensity.

In vivo Biodistribution of Echo-CNPs. *In vivo* biodistribution of Echo-CNPs was obtained by eXplore Optix system (Advanced Research Technologies Inc., Montreal, Canada) at 10 μW of laser power with 0.3 s per imaging point. In brief, Flamma™-labelled Echo-CNPs (5 mg/kg) were intravenously injected into SCC7-bearing BALB/c nude mice, and NIRF images were obtained at the specified time points. To

compare the US-triggered tumor accumulation behavior of Echo-CNPs, the destruction mode of US (10 MHz; mechanical index: 0.235; average power: 0.0676 W/cm²) was applied after 3 min of injection for 60 min, and their fluorescence intensity was observed at the same time points as the non-US treated mice. The resulting NIRF intensities of tumor tissues were quantified at the region of interest at tumor site (30 mm²) by eXplore Optix system software. After 48 h post-injection, tumor and major organs were extracted, and *ex vivo* images were obtained by IVIS Spectrum imaging system (Caliper Life Sciences, Hopkinton, MA). The residual NIRF intensities of organs were quantified by IVIS Spectrum imaging system software.

Fluorescence Imaging in Tumor Tissue. Subcutaneous SCC7 tumor-bearing C3H/HeN mice (n=3, 25-30 g) was used for fluorescence imaging of the tumor tissue. In order to visualize Echo-CNPs and the drug distribution within the tumor tissue, Nile-red was loaded into flamma™ labeled Echo-CNPs as a model drug using the same method for DTX formulation. To evaluate the US-dependent drug release profile in tumor tissue, 100 % power of US (10 MHz; mechanical index: 0.235; average power: 0.0676 W/cm²) was applied to the tumor site for 5 min, at 3 min post-injection of Echo-CNPs (5 mg/kg). Then, the tumor skin was removed and the tumor tissue was imaged after 10 min of injection by OV-100 *in vivo* fluorescence imaging system (Olympus Co. Ltd., Japan) attached with Cy 5.5 and RFP filter. The tumor tissue of non-US treated mice was also imaged in the same condition after Echo-CNP injection, and the fluorescence intensities of Echo-CNPs were analyzed using OV-100 software.

Therapeutic Efficacy of DTX loaded Echo-CNPs (DTX- Echo-CNPs). To verify therapeutic effects of DTX-loaded Echo-CNPs (DTX-Echo-CNPs), 1×10⁶ of SCC-7 cells were subcutaneously inoculated to C3H/HeN male mice (5.5 week, 25 - 30 g) for the tumor model. For tumor treatment, mice were divided into 4 groups: (1) saline, (2) free DTX and (3) DTX-Echo-CNPs and, (4) DTX- Echo-CNPs with US irradiation. When the tumor volumes were approximately 15-20 mm³, (1) saline, (2) free DTX and (3) DTX-Echo-CNPs were administered via tail vein injection (10 mg/kg of DTX) to each group every 3 days for 12 days. For the US irradiation group, bubble destruction process (10 MHz; mechanical index: 0.235; average power: 0.0676 W/cm²) was conducted using Vevo770® system after 3 min of DTX- Echo-CNPs injection. The tumor volumes were measured using caliper every 3 days and calculated using the formula, width×length×height×1/2, for 15 days. After therapy, all mice were sacrificed and tumors were extracted.

Tumor tissues were fixed with 4% paraformaldehyde and embedded into paraffin to be sectioned. The histological changes of tumor tissues were evaluated using hematoxylin-eosin (H&E) staining according to the manufacturer's protocol.

Supplementary Material

Supplementary Figures 1-3.

<http://www.thno.org/v05p1402s1.pdf>

Acknowledgements

This study was funded by the GRL Project (NRF-2013K1A1A2A02050115), the GiRC (NRF-2012K1A1A2A01055811), and the Intramural Research Program of KIST.

Competing Interests

The authors have declared that no competing interest exists.

References

- Rim HP, Min KH, Lee HJ, Jeong SY, Lee SC. pH-Tunable calcium phosphate covered mesoporous silica nanocontainers for intracellular controlled release of guest drugs. *Angewandte Chemie*. 2011; 50: 8853-7.
- Son S, Kim WJ. Biodegradable nanoparticles modified by branched polyethyleneimine for plasmid DNA delivery. *Biomaterials*. 2010; 31: 133-43.
- Son S, Namgung R, Kim J, Singha K, Kim WJ. Bioreducible polymers for gene silencing and delivery. *Accounts of chemical research*. 2012; 45: 1100-12.
- Cheng Z, Al Zaki A, Hui JZ, Muzykantov VR, Tsourkas A. Multifunctional nanoparticles: cost versus benefit of adding targeting and imaging capabilities. *Science*. 2012; 338: 903-10.
- Son S, Singha K, Kim WJ. Bioreducible BPEI-SS-PEG-cNGR polymer as a tumor targeted nonviral gene carrier. *Biomaterials*. 2010; 31: 6344-54.
- Lao J, Madani J, Puertolas T, Alvarez M, Hernandez A, Pazo-Cid R, et al. Liposomal Doxorubicin in the treatment of breast cancer patients: a review. *Journal of drug delivery*. 2013; 2013: 456409.
- Reynolds JG, Geretti E, Hendriks BS, Lee H, Leonard SC, Klinz SG, et al. HER2-targeted liposomal doxorubicin displays enhanced anti-tumorigenic effects without associated cardiotoxicity. *Toxicol Appl Pharm*. 2012; 262: 1-10.
- Hernot S, Klibanov AL. Microbubbles in ultrasound-triggered drug and gene delivery. *Adv Drug Deliver Rev*. 2008; 60: 1153-66.
- Sanna V, Pintus G, Bandiera P, Anedda R, Punzoni S, Sanna B, et al. Development of Polymeric Microbubbles Targeted to Prostate-Specific Membrane Antigen as Prototype of Novel Ultrasound Contrast Agents. *Mol Pharmaceut*. 2011; 8: 748-57.
- Borden MA, Zhang H, Gillies RJ, Dayton PA, Ferrara KW. A stimulus-responsive contrast agent for ultrasound molecular imaging. *Biomaterials*. 2008; 29: 597-606.
- Mayer CR, Geis NA, Katus HA, Bekeredian R. Ultrasound targeted microbubble destruction for drug and gene delivery. *Expert opinion on drug delivery*. 2008; 5: 1121-38.
- Mitragotri S. Innovation - Healing sound: the use of ultrasound in drug delivery and other therapeutic applications. *Nat Rev Drug Discov*. 2005; 4: 255-60.
- Miller DL, Smith NB, Bailey MR, Czarnota GJ, Hynynen K, Makin IRS, et al. Overview of Therapeutic Ultrasound Applications and Safety Considerations. *J Ultras Med*. 2012; 31: 623-34.
- Suzuki R, Oda Y, Utoguchi N, Maruyama K. Progress in the development of ultrasound-mediated gene delivery systems utilizing nano- and microbubbles. *J Control Release*. 2011; 149: 36-41.
- Ibsen S, Benchimol M, Simberg D, Schutt C, Steiner J, Esener S. A novel nested liposome drug delivery vehicle capable of ultrasound triggered release of its payload. *J Control Release*. 2011; 155: 358-66.
- Ferrara KW, Borden MA, Zhang H. Lipid-Shelled Vehicles: Engineering for Ultrasound Molecular Imaging and Drug Delivery. *Accounts of chemical research*. 2009; 42: 881-92.
- Krupka TM, Solorio L, Wilson RE, Wu HP, Azar N, Exner AA. Formulation and Characterization of Echogenic Lipid-Pluronic Nanobubbles. *Mol Pharmaceut*. 2010; 7: 49-59.
- Marxer EEJ, Brussler J, Becker A, Schummelfeder J, Schubert R, Nimsky C, et al. Development and characterization of new nanoscaled ultrasound active lipid dispersions as contrast agents. *Eur J Pharm Biopharm*. 2011; 77: 430-7.

19. Yin TH, Wang P, Zheng RQ, Zheng BW, Cheng D, Zhang XL, et al. Nanobubbles for enhanced ultrasound imaging of tumors. *Int J Nanomed.* 2012; 7: 895-904.
20. Rapoport N, Gao Z, Kennedy A. Multifunctional nanoparticles for combining ultrasonic tumor imaging and targeted chemotherapy. *J Natl Cancer Inst.* 2007; 99: 1095-106.
21. Shiraishi K, Endoh R, Furuhashi H, Nishihara M, Suzuki R, Maruyama K, et al. A facile preparation method of a PFC-containing nano-sized emulsion for theranostics of solid tumors. *Int J Pharm.* 2011; 421: 379-87.
22. Solans C, Izquierdo P, Nolla J, Azemar N, Garcia-Celma M.J. Nano-emulsions. *curr opin colloid interface sci.* 2004; 10: 102-110.
23. Jian J, Liu C, Gong Y, Su L, Zhang B, Wang Z, et al. India ink incorporated multifunctional phase-transition nanodroplets for photoacoustic/ultrasound dual-modality imaging and photoacoustic effect based tumor therapy. *Theranostics.* 2014; 4: 1026-38.
24. Javadi M, Pitt WG, Tracy CM, Barrow JR, Willardson BM, Hartley JM, Tsosie NH. Ultrasonic gene and drug delivery using eLiposomes. *J Control Release.* 2013; 167: 92-100.
25. Javadi M, Pitt WG, Belnap DM, Tsosie NH, Hartley JM. Encapsulating nanoemulsions inside eLiposomes for ultrasonic drug delivery. *Langmuir.* 2012; 28: 14720-9.
26. Min HS, Son S, Lee TW, Koo H, Yoon HY, Na JH, et al. Liver-Specific and Echogenic Hyaluronic Acid Nanoparticles Facilitating Liver Cancer Discrimination. *Adv Funct Mater.* 2013; 23: 5518-29.
27. Kim JH, Kim YS, Park K, Lee S, Nam HY, Min KH, et al. Antitumor efficacy of cisplatin-loaded glycol chitosan nanoparticles in tumor-bearing mice. *J Control Release.* 2008; 127: 41-9.
28. Lee SJ, Park K, Oh YK, Kwon SH, Her S, Kim IS, et al. Tumor specificity and therapeutic efficacy of photosensitizer-encapsulated glycol chitosan-based nanoparticles in tumor-bearing mice. *Biomaterials.* 2009; 30: 2929-39.
29. Lee SJ, Koo H, Jeong H, Huh MS, Choi Y, Jeong SY, et al. Comparative study of photosensitizer loaded and conjugated glycol chitosan nanoparticles for cancer therapy. *J Control Release.* 2011; 152: 21-9.
30. Yoon HY, Son S, Lee SJ, You DG, Yhee JY, Park JH, et al. Glycol chitosan nanoparticles as specialized cancer therapeutic vehicles: Sequential delivery of doxorubicin and Bcl-2 siRNA. *Sci Rep-Uk.* 2014; 4.
31. Son S, Min HS, You DG, Kim BS, Kwon IC. Echogenic nanoparticles for ultrasound technologies: Evolution from diagnostic imaging modality to multimodal theranostic agent. *Nano Today.* 2014; 9: 525-40.
32. Carson AR, McTiernan CF, Lavery L, Grata M, Leng XP, Wang JJ, et al. Ultrasound-Targeted Microbubble Destruction to Deliver siRNA Cancer Therapy. *Cancer Res.* 2012; 72: 6191-9.
33. Liu HL, Fan CH, Ting CY, Yeh CK. Combining Microbubbles and Ultrasound for Drug Delivery to Brain Tumors: Current Progress and Overview. *Theranostics.* 2014; 4: 432-44.
34. Kim JH, Kim YS, Kim S, Park JH, Kim K, Choi K, et al. Hydrophobically modified glycol chitosan nanoparticles as carriers for paclitaxel (Reprinted from *Journal of Controlled Release*, vol 109, pg 1, 2005). *J Control Release.* 2006; 111: 228-34.